

ARTICLE

Received 4 Dec 2013 | Accepted 26 Mar 2014 | Published 29 Apr 2014

DOI: 10.1038/ncomms4723

OPEN

Siple Dome ice reveals two modes of millennial CO₂ change during the last ice age

Jinho Ahn¹ & Edward J. Brook²

Reconstruction of atmospheric CO₂ during times of past abrupt climate change may help us better understand climate-carbon cycle feedbacks. Previous ice core studies reveal simultaneous increases in atmospheric CO₂ and Antarctic temperature during times when Greenland and the northern hemisphere experienced very long, cold stadial conditions during the last ice age. Whether this relationship extends to all of the numerous stadial events in the Greenland ice core record has not been clear. Here we present a high-resolution record of atmospheric CO₂ from the Siple Dome ice core, Antarctica for part of the last ice age. We find that CO₂ does not significantly change during the short Greenlandic stadial events, implying that the climate system perturbation that produced the short stadials was not strong enough to substantially alter the carbon cycle.

¹School of Earth and Environmental Sciences, Seoul National University, Seoul 151742, Korea. ²College of Earth, Ocean and Atmospheric Sciences, Oregon State University, Corvallis, Oregon 97331, USA. Correspondence and requests for materials should be addressed to J.A. (email: jinhoahn@snu.ac.kr).

Ice core records from Greenland reveal a detailed history of abrupt climate change during the last glacial period. Warm and cold periods (interstadial and stadial, respectively) repeated on millennial timescales but rapid switches between the two happened in decades^{1–4}. Antarctic ice core records, however, reveal gradual warming during Greenlandic stadials and cooling during interstadials^{5,6}. The out-of-phase interhemispheric climate relationship is usually referred to as the ‘bipolar seesaw’⁷ and the most popular hypothesis for the control mechanism includes reorganization of ocean-atmosphere circulation and change in meridional heat transport, possibly caused by fresh water input into the North Atlantic^{8–10}.

Reconstruction of atmospheric CO₂ during abrupt climate change events may help us better understand climate-carbon cycle feedbacks and provide data for testing carbon cycle models under variety of boundary conditions. Existing Antarctic ice core records show CO₂ increases during long Greenlandic stadials, which are also accompanied by major Antarctic warmings^{11,12}. Ventilation of CO₂-rich deep water in the Southern Ocean may have controlled ocean-atmosphere carbon exchange and therefore atmospheric CO₂ concentration¹³. Marine sediment records from the Southern Ocean indicate increased opal flux¹⁴ and reduced stratification¹⁵ during the Younger Dryas event and the long stadial preceding the Bølling-Allerød event^{14,15}, both times of rising CO₂, and can be interpreted as a record of increased upwelling and CO₂ outgassing in the Southern Ocean^{14,15}. During the same time intervals, the Atlantic meridional overturning circulation (AMOC) was reduced and the Antarctic temperature gradually increased^{16,17}. During the long stadials of

the last ice age, marine sediment records indicate shoaled AMOC¹⁸ and increased opal flux¹⁴ in the Southern Ocean, although the chronology of the proxy for the latter is not well constrained. The shoaling of AMOC likely coincided with reduction in AMOC strength that might have caused reduction in northward oceanic heat transport, the gradual warming in Antarctica and CO₂ outgassing from the Southern Ocean during the long stadials^{10,14}, analogous to the early stage of the last deglacial Antarctic warming and CO₂ increase^{14,19,20}.

High-resolution records from the EPICA Dronning Maud Land (EDML) ice core in east Antarctica show the ‘bipolar seesaw’ operated not only during the major long stadials but also during other short ones, and that stadial duration is positively correlated with the magnitude of the temperature increase in Antarctica. These observations support the hypothesis of reduction in AMOC during both long and short stadials²¹, although there is no clear marine evidence of AMOC reduction during each of the short stadials, perhaps owing to insufficient data resolution and/or chronology⁶.

By analogy to the relationship between CO₂ and major Antarctic warmings/long Greenlandic stadials, we might expect small CO₂ increases during the small Antarctic warmings/short Greenlandic stadials. However, atmospheric CO₂ change during the short stadials is not well resolved in existing ice core records owing to low temporal data resolution (280–570 years^{11,12,22}).

We investigate CO₂ variations during the short Greenlandic stadials, with a multi-decadal to centennial CO₂ record with a mean sampling resolution of 95 years, from the Siple Dome ice core, Antarctica. Our new results cover the time interval of

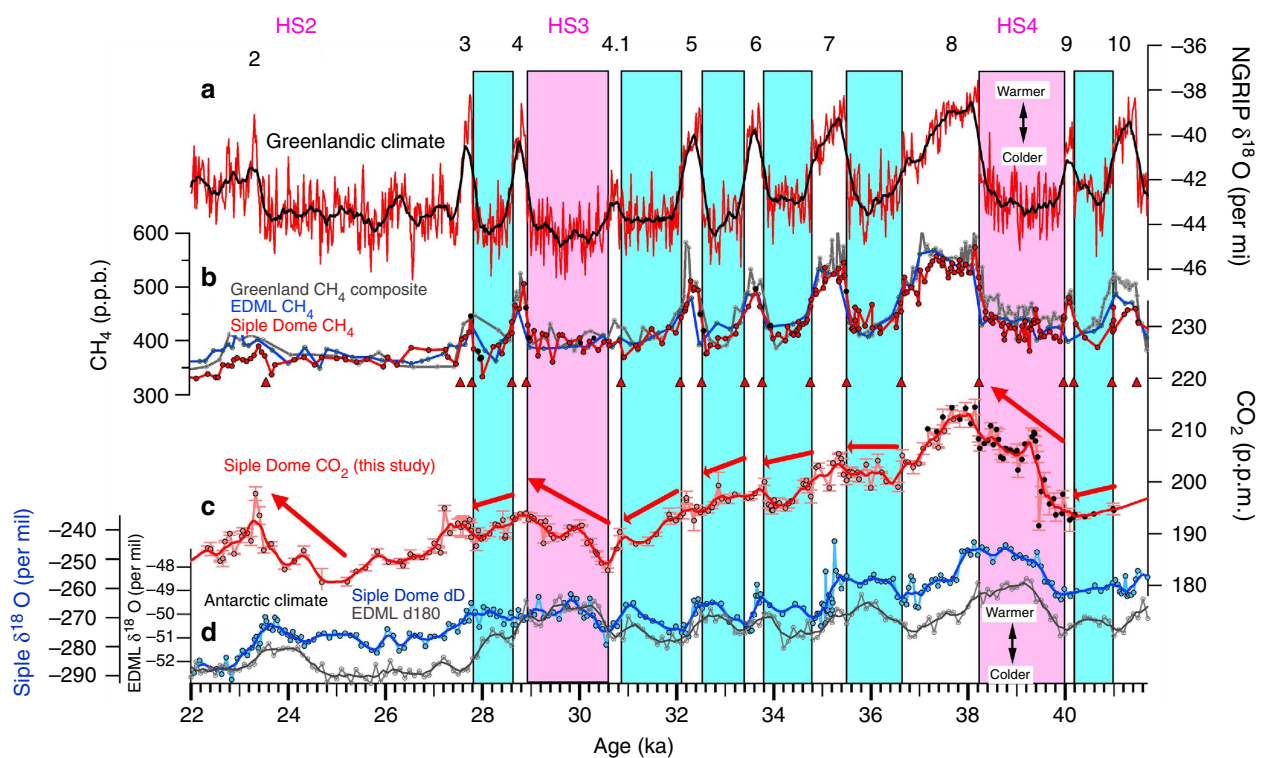


Figure 1 | High-resolution CO₂ and climate records during abrupt climate change during the last ice age. (a) Greenlandic isotopic temperature record from the NGRIP ice core⁵⁷. Black numbers represent Dansgaard-Oeschger events. HS stands for Heinrich stadial, indicating long stadials that include Heinrich events. (b) Atmospheric CH₄ records from Greenland (grey)²¹, Siple Dome (red)²⁴ and EDML (blue)²¹ ice cores. Black dots are new Siple Dome CH₄ data (this study). Red triangles indicate age control points. (c) Atmospheric CO₂ record from Siple Dome, Antarctica ice core (this study). Red line represents 300-year running means of the CO₂ record. Black dots are published records²³. (d) Antarctic temperature proxy records from Siple Dome (dark blue)²⁴ and EDML (grey)²¹ ice cores. All the ages are synchronized on Greenland Ice Core Chronology 2005 (GICC05) timescale. Blue and pink boxes indicate time intervals of short and long stadials (Greenlandic cold spans), respectively. During those stadials, Antarctic temperature increased.

Greenlandic abrupt climate events (Dansgaard-Oeschger or DO events) DO2–7 and our sampling resolution is sufficient to examine CO₂ trends during the short stadials lasting for 800–1200 years. Combined with recently published high-resolution data for DO8–10 from the same core²³, we constructed a complete high-resolution CO₂ record from 22 to 41 ka.

Results

Natural smoothing of gas records in the Siple Dome ice core. Snow accumulation rates at the Siple Dome are relatively high, and therefore smoothing of gas records by diffusion and gradual bubble close-off in the firm (unconsolidated snow layer on the top of ice sheet) is relatively small²⁴. The high snow accumulation rates also result in a small uncertainty in the relative timing between gas ages and ice ages (Δ age)²⁵, allowing better comparison of gas records with temperature proxy records²⁴. A firm densification model for Siple Dome shows Δ age of 500–1000 years during the 22–41-ka period²⁴. Because the width of the gas age distribution at half-height is typically about 10% of Δ age^{25–28}, we estimate the gas age distribution of the Siple Dome record to be <100 years during the time interval of study. The sharp increases in the Siple Dome CH₄ record (Fig. 1) clearly confirm that the smoothing of gas records is minimal on multi-centennial timescales and supports our estimation of smoothing of the Siple Dome CO₂ record.

Two modes of CO₂ change during Greenlandic stadials. As shown in Fig. 1, we observe small CO₂ variations of ~5 p.p.m. on centennial timescales during the short stadials. A 300-year running mean (red curve) removes these features (Fig. 1), illustrating that CO₂ change was negligible on multi-centennial timescales. We observe small decreases on longer timescales during most of the short stadials (Fig. 1), but these are part of a long-term trend. After detrending it becomes clear that the CO₂ change associated with short stadials themselves is insignificant (Fig. 2a). In contrast, we observe CO₂ increases during the long stadials, confirming previous results from different Antarctic ice cores^{11,12,22,29} (Fig. 2a). The isotopic temperature proxy (δD_{ice}) from the Siple Dome ice core shows small Antarctic warmings during most of the short stadials (Fig. 2b) and confirms previous results from the EDML ice core²¹, implying that the small Antarctic warmings during the short stadials are not only local features but at least of larger regional extent because Siple Dome is located in the Pacific sector, while the EDML core is in the Atlantic sector in Antarctica. Combining the Siple Dome CO₂ and climate records, we plot the time evolution of CO₂ versus the temperature proxy (δD_{ice}) anomalies during Greenlandic stadials or Antarctic warmings, using the detrended Siple Dome CO₂ and temperature proxy records for short stadials (Fig. 2c). We find that CO₂ and δD_{ice} anomalies are not significantly correlated during the short stadials (average $r=0.0$), but positively correlated during the long stadials (average $r=0.84$) (Fig. 2c). A slight temperature decrease in the Siple Dome δD_{ice} between DO9 and 10 is not confirmed in the EDML isotopic temperature (δO_{ice}) record²¹ and excluded in our calculation. We note that Siple Dome isotopic temperature (δD_{ice}) between DO3 and 4 increases, but at EDML it decreases, presumably owing to local effects. Our finding of the two different modes of CO₂ change during Greenlandic stadials for the period 22–41 ka is consistent with the results of a recent, lower resolution study of CO₂ variations from 38 to 115 ka¹², which shows <5 p.p.b. variations in CO₂ during the short stadial events of marine isotope stage 3.

Discussion

The small-to-insignificant CO₂ change during the short stadials may imply that AMOC perturbations happened at these events

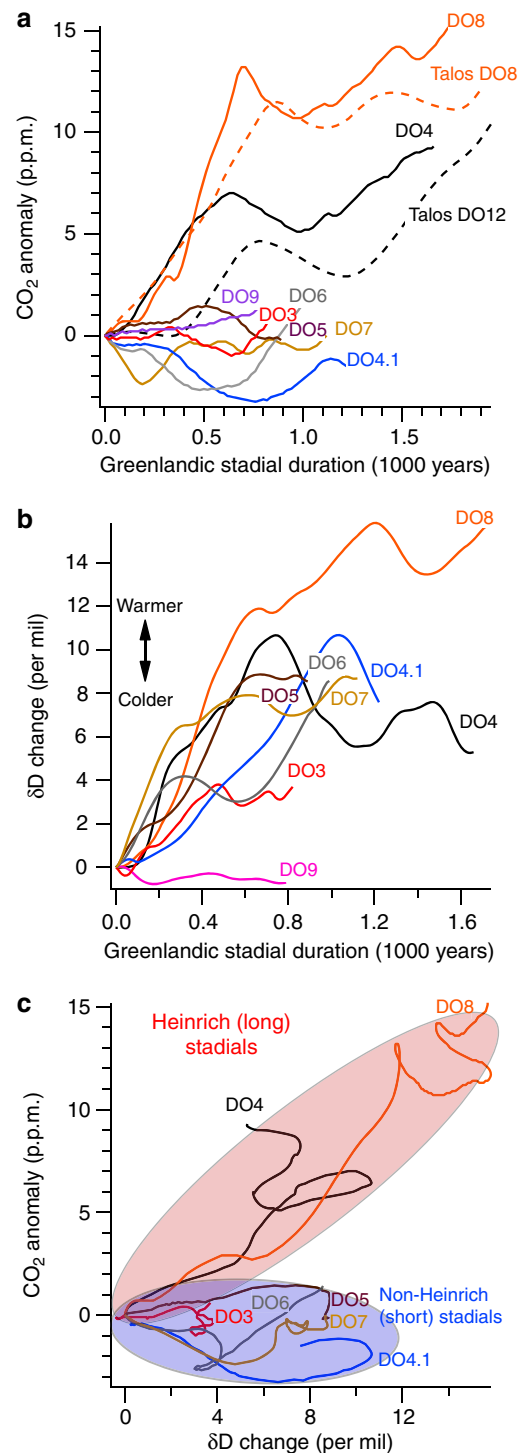


Figure 2 | Time evolution of CO₂ and Antarctic isotope temperature during Greenlandic stadials. (a) CO₂ change during Greenlandic stadials from Siple Dome (solid lines) and Talos Dome (dashed lines)¹² ice core records. DO numbers indicate DO warmings at the end of the stadials. (b) Antarctic temperature proxy record during stadials from Siple Dome ice core²⁴. (c) Time evolution of atmospheric CO₂ versus isotopic temperature anomalies during stadials. Derived from (a,b). The pale red and blue ellipses indicate records for Heinrich (long) and non-Heinrich (short) stadials, respectively. Three hundred-year running means are used for both CO₂ and isotopic temperature proxy records. In order to remove multi-millennial changes during short Greenlandic stadials, the Siple Dome CO₂ and isotopic temperature records are detrended.

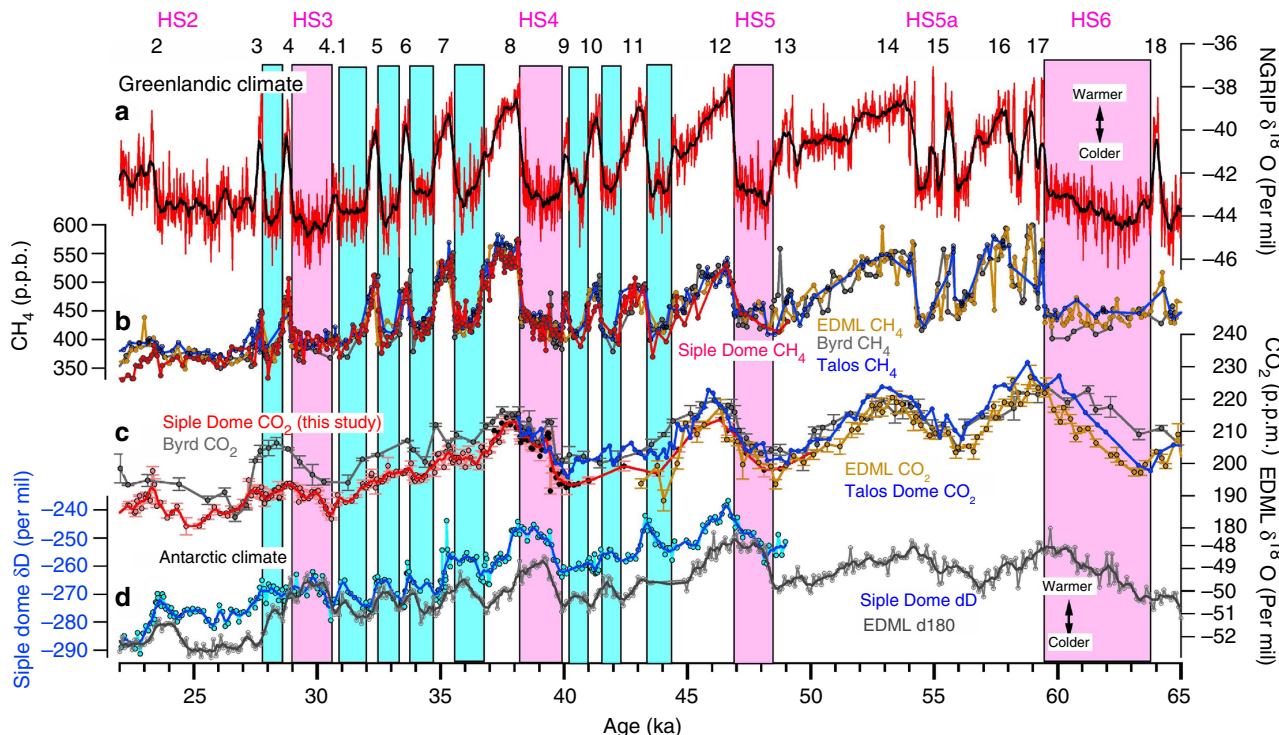


Figure 3 | Atmospheric CO₂ and climate records from multiple ice cores. (a–d) Ice core records extended from Fig. 1. Siple Dome CO₂ and CH₄ records are compared with existing low-resolution records from EPICA EDML^{12,21}, Byrd¹¹ and Talos^{11,58} ice cores, Antarctica. Age intervals for HS2 and HS5a are not well constrained owing to chronological uncertainty in the paleoproxy records.

Table 1 | Gas age tie points for Siple Dome ice core.

Event	Siple Dome depth (m)	GISP2 age (ka) ²⁴	GICC05 age (b2k) ⁵⁵	Age difference
CH ₄ rise associated with				
DO2 onset	739.50	23.93	23.54	-0.39
DO3 end	757.90	27.61	27.54	-0.07
DO3 onset	760.62	28.02	27.78	-0.24
DO4 end	765.80	28.78	28.60	-0.18
DO4 onset	767.81	29.19	28.90	-0.29
DO4.1 onset	780.84	31.09	30.85	-0.24
DO5 end	784.70	31.65	32.07	0.42
DO5 onset	789.03	32.50	32.51	0.01
DO6 end	793.60	33.13	33.40	0.27
DO6 onset	795.03	33.73	33.76	0.03
DO7 end	803.70	34.59	34.75	0.16
DO7 onset	809.94	35.54	35.50	-0.04
DO8 end	816.00	36.31	36.62	0.31
DO8 onset	825.55	38.49	38.22	-0.27
DO9 end	837.40	40.01	39.96	-0.05
DO9 onset	838.32	40.12	40.17	0.05
DO10 end	841.00	40.47	40.96	0.49
DO10 onset	845.99	41.09	41.47	0.38
DO11 end	849.90	41.77	42.27	0.50
DO11 onset	855.28	42.82	43.42	0.60
DO12 end	860.10	43.85	44.34	0.49
DO12 onset	871.77	46.36	46.87	0.51

but were too short to result in a change in atmospheric CO₂. If this were the case, we would expect to observe no CO₂ increase during the first 800–1200 years of the long stadials, because duration of the short stadials ranges 800–1200 years. However, we observe that CO₂ increases from the beginning of the long

Greenlandic stadials predating DO8 and DO4 (Fig. 2a). The time lag of CO₂ relative to the isotopic signal during Greenlandic stadials predating DO12 and 17 from other ice core records appears small as well^{11,12}. However, we cannot clearly rule out the possibility of a time lag of several centuries (Fig. 3). In addition, there is some ambiguity about the start of the long stadial predating DO4, which is conventionally defined by the end of a small temperature proxy peak (DO4.1)²¹. We follow convention here, but note that additional high-resolution data from other long stadial events will be needed to further address the question of when CO₂ starts to rise during events of this type. The above observation suggests that climate perturbations associated with the long and short stadials are different. Cave deposits reveal less weakening in the Asian monsoon³⁰ and less intense South American monsoon³¹ during the short stadials compared with the long stadials, suggesting that the perturbation to the climate system related to the short stadial events in Greenland was weaker than for the long ones. A comparison of Antarctic ice core climate records with a thermodynamic model also indicates that the long stadials were caused by a stronger climate perturbation than short ones³². Finally, although it is not conclusive, δ¹³C in benthic foraminifera from North Atlantic sediment cores indicates less shoaling of AMOC during short stadials than that during the long stadials³³. Thus it is likely that strength of the climate perturbation is related to change in atmospheric CO₂ during the Greenlandic stadials. Massive iceberg discharge events in the North Atlantic (Heinrich events) occurred within time intervals of the long stadials. The Heinrich events could have increased fresh water forcing into the North Atlantic and also caused large perturbations to atmospheric circulation (for example, southward movement of the ITCZ³⁴). However, multiple studies suggest that the Heinrich events lag onsets of long stadials^{35,36}, although exact timing of those events within the stadials is not well constrained^{37,38}.

The control mechanisms for the two CO₂ modes may exist in oceanic processes such as AMOC reduction and consequent upwelling in the Southern Ocean. Those oceanic processes can be linked by change in vertical salinity transport and stratification in the Southern Ocean³⁹ and/or latitudinal shift of Southern Hemisphere Westerlies^{14,40} and/or strength of the Southern Hemisphere Westerlies^{41–43}. Although we cannot pinpoint a precise oceanic mechanism, we speculate that the weakening in AMOC during the short stadials might have not been sufficient to cause enough of a change in upwelling to impact atmospheric CO₂. Marine proxy data for upwelling in the Southern Ocean do not clearly show strong peaks in between long stadials that bracket several short stadials¹⁴, supporting this hypothesis.

Other potential oceanic mechanisms that change CO₂ outgassing include variations in sea ice extent and changes in iron fertilization in the Southern Ocean⁴⁴. Sea-salt-Na may be a proxy for sea ice extent, but Siple Dome, Dome C and EDML ice core records do not show significant differences between long and short Greenlandic stadials^{44,45}. Proxy records for the Fe-flux (non-sea-salt Ca) from Dome C and EDML cores show highly reduced Fe-flux during several long Greenlandic stadials that predate DO8, but after DO8 the reduction during long stadials is not larger than that during short stadials⁴⁴. Thus a difference in iron fertilization in the Southern Ocean is not likely the main cause of the two modes in CO₂ change.

Atmospheric CO₂ can be also controlled by exchange of land carbon. Terrestrial carbon is mostly affected by temperature and precipitation because they both control vegetation and organic carbon in soil. Compared with interstadials, paleoproxy data for both short and long stadials indicate colder and dryer conditions in the northern hemisphere, and warmer and wetter conditions in the southern hemisphere, although the magnitude of those changes depends on the type of stadials⁶. However, model simulations predict either a decrease^{46,47} or increase⁴⁸ in land carbon during the stadials. Although we cannot rule out terrestrial control on the two modes of CO₂ change, we suggest that the control mechanism exists more likely in the ocean rather than on land, because we have supporting evidence for an oceanic CO₂ source during the long stadials in the last deglacial period^{14,15,49,50}.

In principle, the lack of change in atmospheric CO₂ could also result from compensating changes in sources (for example, coincident terrestrial uptake and oceanic release) as predicted in models of AMOC shutdown and carbon cycle response^{46,47,51}. However, the global impact of short stadials on the terrestrial biosphere was probably small, given that paleoproxy records indicate weaker terrestrial climate perturbations during the short Greenlandic stadials compared with the long ones^{30,31} as discussed above. Thus, terrestrial uptake balancing oceanic release during the short Greenlandic stadials is not likely the main explanation for the lack of CO₂ response.

Our new high-resolution record defines two modes of millennial scale CO₂ change during stadial events in the northern hemisphere that depend on the nature of the Greenlandic stadial. During short Greenlandic stadials, those not associated with Heinrich events, it is likely that the impact on ocean circulation was not sufficient to release CO₂ from deep ocean to the atmosphere. The lack of correlation between CO₂ and Antarctic temperature change during the short stadials implies that links between Antarctic climate change and high-latitude northern hemisphere climate may have been controlled by shallow oceanic and/or atmospheric processes, while CO₂ change was controlled by deep oceanic and Southern Ocean processes.

Methods

CO₂ concentration measurement. For CO₂ analysis at the Oregon State University, samples were placed in a double-walled stainless steel chamber at

–35 °C, cooled using cold ethanol circulation between the walls, evacuated for 13 min and then crushed with steel pins. Air liberated from the ice was dried in a cold stainless steel coil at –85 °C and then trapped in ~6 cm³ stainless steel sample tubes at –262 °C. After warming the trapped air to room temperature, the CO₂ mixing ratio was measured with an Agilent 6890N Gas Chromatograph (GC) with a flame ionization detector, with nickel catalyst conversion of CO₂ to CH₄ before measurement. Daily calibration curves used several measurements of standard air with 197.54 p.p.m. CO₂ (WMOX2007 CO₂ mole fraction scale). Daily corrections for the dry extraction and GC analysis were done using several standard airs (197.54 p.p.m.) that were introduced over the ice samples and trapped in sample tubes mimicking the procedure of the air samples from ice. We compared 2–5 replicates from the same depths. Details of the methods are described in ref. 52. The s.e. for replicates from the same depth averaged 0.6 p.p.m. for the Siple Dome ice. The excellent agreement among the replicates were achieved by careful trimming of the ice surface and improved analytical techniques⁵² since our early analysis for the same core a decade ago at Scripps Institution of Oceanography⁵³.

CH₄ concentration measurement. CH₄ analysis was separately performed at the Oregon State University⁵⁴. Duplicate samples with a weight of ~60 g for each were analysed for each depth interval. Samples were placed in cold glass flasks bathed in an ethanol bath at –64.5 °C. The flasks with the ice samples were evacuated for 1 h. The flasks valves were closed and then the ice was melted in a warm water bath. After melting, the flasks were submerged in the cold ethanol bath to refreeze the ice melt. Air liberated from each ice sample was analysed four times with an Agilent 6890N GC with a flame ionization detector. Data are reported on the NOAA04 methane concentration scale.

Synchronization of ice core records. Our CO₂ record from the Siple Dome core is synchronized with NGRIP (North Greenland Ice Core Project) ice ages on the Greenland Ice Core Chronology 2005 (GICC05) timescale⁵⁵ using abrupt CH₄ changes that are near synchronous with abrupt Greenlandic climate change⁵⁶. We used updated CH₄ records to make better synchronization. The CH₄ data resolution is 82 and 232 years for 23.5–42.3 and 42.3–46.9 ka, respectively. The GICC05 timescale is based on layer counting of Greenland ice cores and agrees well with other absolute ages such as cave deposit records⁵⁵. At DO2, the correlation between CH₄ increase and Greenlandic warming is not clear, and thus we correlate Siple Dome CH₄ with the NGRIP CH₄ record. The age tie points are listed in Table 1 and their uncertainty is controlled primarily by the CH₄ data resolution. The age differences were linearly interpolated at depths between the tie points, and we reconstructed new ages at those depths by adding the calculated difference to the original ages²⁴. Synchronized ice ages were determined using published estimates of ice age-gas age difference²⁴.

References

- Dansgaard, W. *et al.* Evidence for general instability of past climate from a 250-kyr ice-core record. *Nature* **364**, 218–220 (1993).
- Groote, P. M., Stuiver, M., White, J. W. C., Johnsen, S. J. & Jouzel, J. Comparison of oxygen isotope records from the GISP2 and GRIP Greenland ice cores. *Nature* **366**, 552–554 (1993).
- Steffensen, J. P. *et al.* High-resolution Greenland ice core data show abrupt climate change happens in few years. *Science* **321**, 680–684 (2008).
- Thomas, E. R. *et al.* Anatomy of a Dansgaard-Oeschger warming transition: high-resolution analysis of the North Greenland Ice Core Project ice core. *J. Geophys. Res.* **114**, D08102 (2009).
- Blunier, T. & Brook, E. J. Timing of millennial-scale climate change in Antarctica and Greenland during the last glacial period. *Science* **291**, 109–112 (2001).
- Clement, A. C. & Peterson, L. C. Mechanisms of abrupt climate change of the last glacial period. *Rev. Geophys.* **46**, RG4002 (2008).
- Broecker, W. S. Paleocan circulation during the last deglaciation: a bipolar seesaw? *Paleoceanography* **13**, 119–121 (1998).
- Crowley, T. J. North Atlantic deep water cools the southern hemisphere. *Paleoceanography* **7**, 489–497 (1992).
- Schmittner, A., Saenko, O. A. & Weaver, A. J. Coupling of the hemispheres in observations and simulations of glacial climate change. *Quat. Sci. Rev.* **22**, 659–671 (2003).
- Stocker, T. F. & Johnsen, S. J. A minimum thermodynamic model for the bipolar seesaw. *Paleoceanography* **18**, 1087 (2003).
- Ahn, J. & Brook, E. J. Atmospheric CO₂ and climate on millennial time scales during the last glacial period. *Science* **322**, 83–85 (2008).
- Bereiter, B. *et al.* Mode change of millennial CO₂ variability during the last glacial cycle associated with a bipolar marine carbon seesaw. *Proc. Natl Acad. Sci. USA* **109**, 9755–9760 (2012).
- Sigman, D. M., Hain, M. P. & Haug, G. H. The polar ocean and glacial cycles in atmospheric CO₂ concentration. *Nature* **466**, 47–55 (2010).
- Anderson, R. F. *et al.* Wind-driven upwelling in the Southern Ocean and the deglacial rise in atmospheric CO₂. *Science* **323**, 1443–1448 (2009).

15. Skinner, L. C., Fallon, S., Waelbroeck, C., Michel, E. & Barker, S. Ventilation of the deep Southern Ocean and deglacial CO₂ rise. *Science* **328**, 1147–1151 (2010).
16. McManus, J. F., Francois, R., Cherardi, J.-M., Keigwin, L. D. & Brown-Leger, S. Collapse and rapid resumption of Atlantic meridional circulation linked to deglacial climate changes. *Nature* **428**, 834–837 (2004).
17. Lynch-Stieglitz, J., Curry, W. B. & Slowey, N. Weaker Gulf stream in the Florida straits during the last glacial maximum. *Nature* **402**, 644–648 (1999).
18. Shackleton, N. J., Hall, M. A. & Vincent, E. Phase relationships between millennial-scale events 64,000–24,000 years ago. *Paleoceanography* **15**, 565–569 (2000).
19. Pedro, J. B., Rasmussen, S. O. & van Ommen, T. D. Tightened constraints on the time-lag between Antarctic temperature and CO₂ during the last deglaciation. *Clim. Past* **8**, 1213–1221 (2012).
20. Parrenin, F. *et al.* CO₂ and Antarctic temperature during the last deglacial warming. *Science* **339**, 1060–1063 (2013).
21. EPICA Community members. One-to-one coupling of glacial climate variability in Greenland and Antarctica. *Nature* **444**, 195–198 (2006).
22. Indermühle, A., Monnin, E., Stauffer, B., Stocker, T. F. & Wahlen, M. Atmospheric CO₂ concentration from 60 to 20 kyr BP from the Taylor Dome ice core, Antarctica. *Geophys. Res. Lett.* **27**, 735–738 (2000).
23. Ahn, J., Brook, E. J., Schmittner, A. & Kreutz, K. Abrupt change in atmospheric CO₂ during the last ice age. *Geophys. Res. Lett.* **39**, L18711 (2012).
24. Brook, E. J. *et al.* Timing of millennial-scale climate change at Siple Dome, West Antarctica, during the last glacial period. *Quat. Sci. Rev.* **24**, 1333–1343 (2005).
25. Schwander, J. *et al.* Age scale of the air in the summit ice: Implication for glacial-interglacial temperature change. *J. Geophys. Res.* **102**, 19483–19493 (1997).
26. Trudinger, C. M. *et al.* Modeling air movement and bubble trapping in firn. *J. Geophys. Res.* **102**, 6747–6763 (1997).
27. Monnin, E. *et al.* Atmospheric CO₂ concentrations over the last glacial termination. *Science* **291**, 112–114 (2001).
28. Ahn, J., Brook, E. J. & Buizert, C. Response of atmospheric CO₂ to the abrupt cooling event 8200 years ago. *Geophys. Res. Lett.* **41**, 604–609 (2014).
29. Ahn, J. & Brook, E. J. Atmospheric CO₂ and climate from 65 to 30 ka B.P. *Geophys. Res. Lett.* **34**, L10703 (2007).
30. Wang, Y. J. *et al.* A high-resolution absolute-dated late Pleistocene monsoon record from Hulu cave, China. *Science* **294**, 2345–2348 (2001).
31. Kanner, L. C., Burns, S. J., Cheng, H. R. & Edwards, L. High-latitude forcing of the South American summer monsoon during the last glacial. *Science* **335**, 570–573 (2012).
32. Margari, V. *et al.* The nature of millennial-scale climate variability during the past two glacial periods. *Nat. Geosci.* **3**, 127–131 (2010).
33. Elliot, M., Labeyrie, L. & Duplessy, J.-C. Changes in North Atlantic deep-water formation associated with the Dansgaard-Oeschger temperature oscillations (60–10 ka). *Quat. Sci. Rev.* **21**, 1153–1165 (2002).
34. Chiang, J. C., Biasutti, M. & Battisti, D. S. Sensitivity of the Atlantic intertropical convergence zone to last glacial maximum boundary conditions. *Paleoceanography* **18**, 1094 (2003).
35. Clark, P., Hostetler, S. W., Pisias, N. G., Schmittner, A. & Meissner, K. J. in *Ocean Circulation: Mechanisms and Impacts*, Vol. 173 (eds Andreas Schmittner, John Chiang & Sidney Hemming) 209–246 (AGU Geophysical Monograph Series, 2007).
36. Marcott, S. *et al.* Ice-shelf collapse from subsurface warming as a trigger for Heinrich events. *Proc. Natl Acad. Sci. USA* **108**, 13415–13419 (2011).
37. Sarnthein, M. *et al.* in *The Northern North Atlantic: A Changing Environment* (eds Schäfer, P., Schlüter, M., Ritzrau, W. & Thiede, J.) 365–410 (Springer, 2001).
38. Hemming, S. Heinrich events: massive late Pleistocene detritus layers of the North Atlantic and their global climate imprint. *Rev. Geophys.* **42**, RG1005 (2004).
39. Schmittner, A., Brook, E. J. & Ahn, J. in *Ocean Circulation: Mechanisms and Impacts* Vol. 173 (eds Andreas Schmittner, John Chiang & Sidney Hemming) 315–334 (AGU Geophysical Monograph Series, 2007).
40. Toggweiler, J. R., Russell, J. L. & Carson, S. R. Midlatitude westerlies, atmospheric CO₂, and climate change during the ice ages. *Paleoceanography* **21**, PA2005 (2006).
41. Tschumi, T., Joos, F. & Parekh, P. How important are Southern Hemisphere wind changes for low glacial carbon dioxide? A model study. *Paleoceanography* **23**, PA4208 (2008).
42. Menviel, L., Timmermann, A., Mouchet, M. & Timm, O. Meridional reorganizations of marine and terrestrial productivity during Heinrich events. *Paleoceanography* **23**, PA4201 (2008).
43. d'Orgeville, M., Sijp, W. P., England, M. H. & Meissner, K. J. On the control of glacial-interglacial atmospheric CO₂ variations by the Southern Hemisphere westerlies. *Geophys. Res. Lett.* **37**, L21703 (2010).
44. Fischer, H. *et al.* Reconstruction of millennial changes in dust emission, transport and regional sea ice coverage using the deep EPICA ice cores from the Atlantic and Indian Ocean sector of Antarctica. *Earth Planet. Sci. Lett.* **260**, 340–354 (2007).
45. Mayewski, P. A. *et al.* State of the Antarctic and Southern Ocean climate system. *Rev. Geophys.* **47**, RG1003 (2009).
46. Bozbiyik, A., Steinacher, M., Joos, F., Stocker, T. F. & Menviel, L. Fingerprints of changes in the terrestrial carbon cycle in response to large reorganizations in ocean circulation. *Clim. Past* **7**, 319–338 (2011).
47. Menviel, L., Timmermann, A., Mouchet, M. & Timm, O. Meridional reorganizations of marine and terrestrial productivity during Heinrich events. *Paleoceanography* **23**, PA1203 (2008).
48. Köhler, P., Joos, F., Gerber, S. & Knutti, R. Simulated changes in vegetation distribution, land carbon storage, and atmospheric CO₂ in response to a collapse of the North Atlantic thermohaline circulation. *Clim. Dynamics* **25**, 689–708 (2005).
49. Schmitt, J. *et al.* Carbon isotope constraints on the deglacial CO₂ rise from ice cores. *Science* **336**, 711–714 (2012).
50. Burke, A. & Robinson, L. F. The Southern Ocean's role in carbon exchange during the last deglaciation. *Science* **335**, 557–561 (2012).
51. Schmittner, A. & Galbraith, E. D. Glacial greenhouse-gas fluctuations controlled by ocean circulation changes. *Nature* **456**, 373–376 (2008).
52. Ahn, J., Brook, E. J. & Howell, K. A high-precision method for measurement of paleoatmospheric CO₂ in small polar ice samples. *J. Glaciol.* **55**, 499–506 (2009).
53. Ahn, J. *et al.* A record of atmospheric CO₂ during the last 40,000 years from the Siple Dome, Antarctica ice core. *J. Geophys. Res.* **109**, D13305 (2004).
54. Mitchell, L. E., Brook, E. J., Sowers, T., McConnell, J. R. & Taylor, K. Multidecadal variability of atmospheric methane, 1000–1800 C.E. *J. Geophys. Res.* **116**, G02007 (2011).
55. Svensson, A. *et al.* A 60 000 year Greenland stratigraphic ice core chronology. *Clim. Past* **4**, 47–57 (2008).
56. Huber, C. *et al.* Isotope calibrated Greenland temperature record over Marine Isotope Stage 3 and its relation to CH₄. *Earth Planet. Sci. Lett.* **243**, 504–519 (2006).
57. North Greenland Ice Core Project members. High-resolution record of Northern Hemisphere climate extending into the last interglacial period. *Nature* **431**, 147–151 (2004).
58. Schüpbach, S., Federer, U., Bigler, M., Fischer, H. & Stocker, T. F. A redefined TALDICE-1a age scale from 55 to 112 ka before present for the Talos Dome ice core based on high-resolution methane measurements. *Clim. Past* **7**, 1001–1009 (2011).

Acknowledgements

We thank Michael Kalk for analytical assistance and the staff of the National Ice Core Lab for ice sampling and curation. We also thank Andreas Schmittner and Luke Skinner for helpful discussions. Financial support was provided by the National Science Foundation Grant OPP 0944764. This work was also supported by Polar Academic Program (PAP, PD12010) of the Korea Polar Research Institution (KOPRI) research grant and Basic Science Research Program through the National Research Foundation of Korea (NRF) funded by the Ministry of Education, Science and Technology (2011-0025242). The data will be available at NSIDC (National Snow and Ice Data Center) and NOAA (National Oceanic and Atmospheric Administration) Palaeoclimatology websites.

Author contributions

J.A. designed and carried out the experiments. All authors interpreted the data and wrote the manuscript.

Additional information

Supplementary Information accompanies this paper at <http://www.nature.com/naturecommunications>

Competing financial interests: The authors declare no competing financial interests.

Reprints and permission information is available online at <http://npg.nature.com/reprintsandpermissions/>

How to cite this article: Ahn, J. & Brook, E.J. Siple Dome ice reveals two modes of millennial CO₂ change during the last ice age. *Nat. Commun.* 5:3723 doi: 10.1038/ncomms4723 (2014).



This work is licensed under a Creative Commons Attribution 3.0 Unported License. The images or other third party material in this article are included in the article's Creative Commons license, unless indicated otherwise in the credit line; if the material is not included under the Creative Commons license, users will need to obtain permission from the license holder to reproduce the material. To view a copy of this license, visit <http://creativecommons.org/licenses/by/3.0/>